JOC*Article*

A DFT Investigation of the Addition Reaction of Monomeric Lithium Enolate Derived from Propiophenone to Propene Oxide: Examination of the Possible Transition Structures

Christian Silvio Pomelli

Dipartimento di Chimica e Chimica Industriale, Università di Pisa, Via Risorgimento 35, 56126 Pisa, Italy

Anna Maria Bianucci

Dipartimento di Scienze Farmaceutiche, Università di Pisa, Via Bonanno 6, 56126 Pisa, Italy

Paolo Crotti* and Lucilla Favero*

Dipartimento di Chimica Bioorganica e Biofarmacia, Università di Pisa, Via Bonanno 33, 56126 Pisa, Italy

lucillaw@farm.unipi.it

Received May 6, 2003

The addition reaction of monomeric lithium enolate (Z)-**1**, derived from propiophenone, to propene oxide **2**, was examined to clarify the exact geometry of the transition state (TS) involved in this type of reaction. The eight possible TSs and the corresponding pathways, four leading to syn γ-hydroxy ketone (γ-HK) **3** and four leading to anti γ-HK **4**, were compared, using the B3LYP/6-31+G(d)//B3LYP/6-31+G(d) theory level in vacuo and in the presence of the reaction solvent (toluene/hexane). In every case, the favored pathway involves a TS where the enolate C=C and the epoxide C−C are in a gauche relationship and where the Li^+ is stabilized by some C−C and C−H σ bonds of epoxide **2**.

Introduction

In the past few years, the addition reaction of lithium enolates, derived from esters and ketones, to epoxides has been the object of some consideration, because it offers a direct route for the synthesis of γ-hydroxy esters (γ-HEs) and ketones (γ-HKs), a very useful class of difunctionalized organic compounds.[1] In fact more complex molecules can be synthesized by using these compounds as synthons, and polysubstituted lactones and tetrahydrofuranes, or related bicyclic, carbocyclic, and heterocyclic compounds, can be obtained by cyclization of γ-HEs and γ-HKs, respectively.[2]

Recently, we introduced in synthesis the reaction of lithium enolates of simple ketones with epoxides in the presence of $LiClO_4$, lanthanide salts, or $Sc(OTf)_3$.[3] When $Sc(OTf)_3$ was used as the catalyst, the addition reaction of lithium enolate (*Z*)-**1**, derived from propiophenone, to propene oxide **2**, in toluene/hexane, afforded a mixture of *syn*-**3** and γ-HK *anti*-**4** with only a slight preference for the anti adduct (*syn*-**3**:*anti*-**4** ratio = 45:55)[3c] (Scheme 1). The reaction was completely regioselective with an exclusive attack of the enolate on the less substituted oxirane carbon. These experimental results were rationalized by admitting transition states such as **5** (leading to the syn adduct **3**) and **6** (leading to the anti adduct **4**),

SCHEME 1

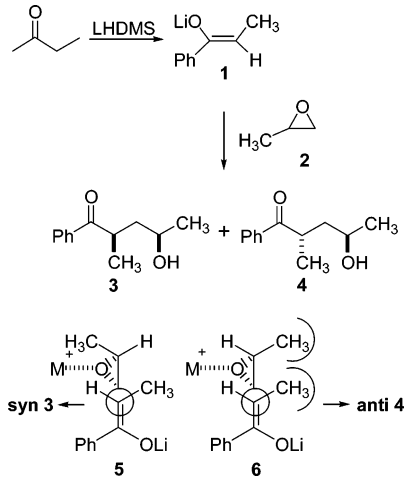

(1) Watanabe, M.; Soai, K. *J. Chem. Soc., Perkin Trans. 1* **1994**, 3125 and references therein.

(2) (a) Harmange, J. C.; Figadère, B. *Tetrahedron*: *Asymmetry* **1993**, *4*, 1711 and references therein. (b) Ellison, R. A. *Synthesis* **1973**, 397. (c) Ho, T. L. *Synth. Commun.* **1974**, *4*, 265. (d) Hudlicky, T.; Price, J. D. *Chem. Rev.* **1989**, *89*, 1467. (e) Bosshard, P.; Eugster, C. H. *Adv. Heterocycl. Chem.* **1966**, *7*, 377.

(3) (a) Chini, M.; Crotti, P.; Favero, L.; Pineschi, M. *Tetrahedron Lett.* **1991**, *32*, 7583. (b) Crotti, P.; Di Bussolo, V.; Favero, L.; Macchia, F.; Pineschi, M. *Tetrahedron Lett.* **1994**, *35*, 6537. (c) Crotti, P.; Di Bussolo, V.; Favero, L.; Pasero, M.; Pineschi, M. *J. Org. Chem.* **1996**, *61*, 9548.

(4) Taylor S. K. *Tetrahedron* **2000**, *56*, 1149 and references therein.

(5) Ziegler T. *Chem. Rev.* **1991**, *91*, 651 and references therein.

10.1021/jo034587m CCC: $27.50
Published on Web 12/10/2003

TABLE 1. Stereoselectivity of the Addition Reaction of Enolate 1 to Epoxide 2

entry	catalyst	*t* (h)	*T* (°C)	*syn*-**3**:*anti*-**4** ratio[a]	yield, %[b]
1[c]	$Sc(OTf)_3$	1	rt	63:37	18
2[c]	$Sc(OTf)_3$	18	rt	45:55	95
3[d]	no catalyst	1	rt		
4[d]	no catalyst	3	rt	43:57	14
5[d]	no catalyst	7	rt	45:55	27
6[d]	no catalyst	24	rt	45:55	30
7[d]	no catalyst	192	rt	45:55	50

[a] The *syn*-**3**/*anti*-**4** ratio was determined by ^{1}H NMR examination of the acetylated crude reaction product (see ref 3c). [b] Yields are based on weight and ^{1}H NMR examination of the crude reaction product. [c] Reference 3c. [d] This work.

similar to the one previously admitted for the corresponding addition reaction of aluminum enolates of esters to epoxides, with the metal (M^+ = $AlMe_3$, Sc^{3+}, Li^+) complexed to the oxirane oxygen.[4] Examination of TS structures **5** and **6** indicates that the reaction should be intrinsically syn diastereoselective, because of the absence, in **5**, of any interaction between the methyl of the enolate and the epoxide, which is present in **6**. The lack of selectivity observed in the addition reaction of enolate (*Z*)-**1** to epoxide **2** was shown to be due to a partial epimerization of the initially formed γ-HK *syn*-**3** under basic reaction conditions.[3c]

To clarify the exact geometry of the transition state effectively involved in this type of reaction, and because of the absence in the literature of any similar study, we thought it valuable to carry out an extensive theoretical study of the addition reaction of the lithium enolate (*Z*)-**1**, derived from propiophenone, to propene oxide **2**. For the sake of simplicity, in our first approach to the study of this reaction, the promoting activity of a metal salt ($LiClO_4$, $Sc(OTf)_3$) was not considered, because the reaction occurs to a sufficient extent also in the absence of the promoting Sc^{3+} species. In fact, the uncatalyzed addition reaction of the lithium enolate (*Z*)-**1** to epoxide **2** afforded the 45:55 mixture of γ-HKs **3** and **4**, as in the presence of $Sc(OTf)_3$, even if with a lower yield and after a longer reaction time (entries 2, 6, and 7, Table 1). Despite the presence of a metal, the enolate counterion Li^+, also in the uncatalyzed protocol, the decidedly slow rate observed for the addition reaction carried out under these conditions could indicate that, contrary to expectations based on the hypothetical TS shown in Scheme 1, the metal (Li^+) has no significant promoting role in this case. The calculations presently under way could turn out to be useful in understanding the exact role of Li^+ in this reaction.

Interestingly, whereas in the uncatalyzed reaction the **3**/**4** ratio did not change in the course of the reaction, in the $Sc(OTf)_3$-catalyzed protocol the **3**/**4** ratio is 63:37 after 1 h, and reaches the final equilibrium value (45:55) only after 18 h (entries 1 and 2, Table 1).

Computational Details

Quantum-chemical computations were carried out with the Gaussian 98 set of programs. Preliminary calculations were performed with use of the HF level of theory with a minimal basis set (STO-3G or 3-21G). The geometrical optimizations of stationary points along the potential energy hypersurface (PES) were performed at the density functional theory level (B3LYP)[5] with the 6-31+G(d) basis set.[6] Berny analytical gradient optimization routines were used for optimization. An eigenvalue following algorithm (Berny algorithm) was used to locate the transition structures (TSs). All stationary points were characterized by frequency calculations to verify that minima and TSs have no, or only one, imaginary frequency. The TSs were localized in several ways: (i) by a scan at the lower theory level (HF/STO-3G or HF/3-21G) and further optimization; (ii) by the use of the STQN method[7] (QST2 or QST3 calculations that contain an appropriate algorithm for the optimization); or (iii) by a combination of (i) and (ii). To determine the two minima connected to a first-order saddle point, we used the scan on PES at the lower theory level (HF/STO-3G or HF/3-21G) and, at the same time, a relax of the saddle point at B3LYP/6-31+G(d), after individualization of the eigenvector corresponding to the negative eigenvalue. Enthalpy, entropy, ZPE, and free energy values were calculated by using the standard expressions for an ideal gas in the canonical ensemble at 298.15 K and 1 atm of pressure.[8] The calculated free energy values in vacuo for all structures (reactants, products, and TSs) were corrected by adding the ZPE and taking away E-TS rotational and translational terms. These thermal and entropic corrections were calculated according to the Ben-Naim scheme for thermochemical properties in the liquid phase.[9] The MP2/6-31+G(d) SP (single point) energy calculations in vacuo were performed on the previously B3LYP/6-31+G(d) optimized structures. The results obtained did not afford any significant differences compared with the corresponding DFT results (extended Table 2 and computational data for all the structures, Supporting Information). The polarized continuum (overlapping spheres) Tomasi model with the integral equation formalism model (IEF-PCM)[10,11] was used to calculate the SP energy of all B3LYP/6-31+G(d) structures optimized in vacuo in the presence of the reaction solvent (toluene/hexane, ϵ = 2.104). In the case of the structure **TS3Ao**, the IEF-PCM was used in the scan of PES to verify the importance of the solvent in the identification of the minimum corresponding to reagents.

Results and Discussion

We took into appropriate consideration all the reasonable TSs, related to the addition reaction of monomeric enolate **1** to epoxide **2**, which could be obtained by varying the following two parameters: (a) the dihedral angle (180° or 60°) between the double bond of the enolate and the C−C bond of the oxirane ring, giving two different situations called **A** (anti relationship, 180°) or **G** (gauche relationship, 60°), and (b) the presence or the absence of a chelation process mediated by the counterion of the enolate (Li^+) between the oxygen of the enolate and epoxide functionality, indicated by the letters **c** (chelated) or **o** (open), respectively. The resulting eight TSs, four

(6) (a) Hariharan, P. C.; Pople, J. A. *Theor. Chim. Acta* **1973**, *28*, 213. (b) Francl, M. M.; Pietro, W. J.; Hehre, W. J.; Binkley, J. S.; Gordon, M. S.; DeFrees, D. J.; Pople, J. A. *J. Chem. Phys.* **1982**, *77*, 3654. (c) Clark, T.; Chandrasekhar, J.; Spitznagel, G. W.; Schleyer, P. v. R. *J. Comput. Chem.* **1983**, *4*, 294. (d) Krishnan, R.; Binkley, J. S.; Seeger, R.; Pople, J. A. *J. Chem. Phys.* **1980**, *72*, 650. (d) Gill, P. M. W.; Johnson, B. G.; Pople, J. A.; Frisch, M. *J. Chem. Phys. Lett.* **1992**, *197*, 499.

(7) Peng, C.; Schlegel, H. B. *Isr. J. Chem.* **1993**, *33*, 449.

(8) McQuarrie, D. A. *Statistical Thermodynamics*; Harper and Row: New York, 1974.

(9) Ben-Naim, A.; Marcus, Y. *J. Chem. Phys* **1984**, *81*, 2016.

(10) (a) Tomasi, J.; Persico, M. *Chem. Rev.* **1994**, *94*, 2027. (b) Cossi, M.; Barone, V.; Cammi, R.; Tomasi, J. *Chem. Phys. Lett.* **1996**, *255*, 327.

(11) (a) Cances, E.; Mennucci, B.; Tomasi, J. *J. Chem. Phys.* **1997**, *107*, 3032. (b) Cossi, M.; Barone, V.; Mennucci, B.; Tomasi, J. *Chem. Phys. Lett.* **1998**, *286*, 253. (c) Mennucci, B.; Cammi, R.; Tomasi, J. *J. Chem. Phys.* **1998**, *109*, 2798.

TABLE 2. $\Delta Ee^{\#}$, ΔEe, $\Delta G^{\#}$, and ΔG (kcal mol^{-1}) for Each Reaction Pathway, with Vacuum and IEF-PCM Solvent Model B3LYP/6-31+G(d) Results

entry	reaction pathway	$\Delta Ee^{\#}$ [a]	$\Delta Ee^{\#}$ [b]	$\Delta Ee^{\#}_{rel}$ [a,c]	$\Delta Ee^{\#}_{rel}$ [b,c]	ΔEe [a]	ΔEe [b]	$\Delta G^{\#}$ [a,d]	ΔG [a,d]	$\Delta G^{\#}_{rel}$ [a,d,e]
1	**7a → TS3Gc → 3a**	+35.60	+36.42	0.00	0.00	-26.97	−26.73	+39.19	−19.81	0.00
2	**7a → TS3Ac → 3b**	+40.22	+40.39	+4.62	+3.97	-9.14	−14.46	+44.98	−4.10	+5.79
3	**7b → TS3Go → 3d**	+25.81	+23.84	+6.65	+6.17	+5.28	−2.67	+27.79	+8.78	+5.87
4	**7a → TS3Ao → 3c**	+46.83	+38.45	+11.23	+2.03	-26.10	−26.05	+49.70	−19.46	+10.51
5	**7a → TS4Gc → 4a**	+42.74	+44.08	+7.14	+7.66	−22.92	−23.24	+46.47	−16.45	+7.28
6	**7a → TS4Ac → 4b**	+40.30	+40.48	+4.70	+4.05	−11.94	−17.00	+45.26	−7.40	+6.07
7	**7b → TS4Go → 4c**	+25.84	+23.76	+6.68	+6.10	+0.59	−5.14	+27.66	+5.03	+5.74
8	**7a → TS4Ao → 4b**	+48.08	+39.54	+12.47	+3.12	−11.94	−17.00	+51.17	−7.40	+11.98
9	**7a → TS′ → I** [f]	+20.96	+18.91			+16.53	+18.41	+18.38	+15.09	
10	**I** [f] **→ TS″ → 7b**	+1.51	+1.11			−0.09	+0.35	+3.75	+2.18	
11	**isolated reag. → 7a**					−21.85	−9.71		−26.93	
12	**isolated reag. → 7b**					−5.41	+9.04		−9.67	

[a] B3LYP/6-31+G(d) vacuum results. [b] B3LYP/6-31+G(d) IEF-PCM results. [c] The difference of the electron energy $Ee^{\#}$ value of the TS of entry 1 (**TS3Gc**) and the electron energy $Ee^{\#}$ value of the TS under examination. [d] The calculated free energy values in vacuo for all structures (reactants, products, and TSs) were corrected by adding the ZPE and taking away E-TS rotational and translational terms. [e] The difference of the corrected free energy $G^{\#}$ value of the TS of entry 1 (**TS3Gc**) and the corrected free energy $G^{\#}$ value of the TS under examination. [f] **I** = Intermediate, see Schemes 3 and 4.

SCHEME 2

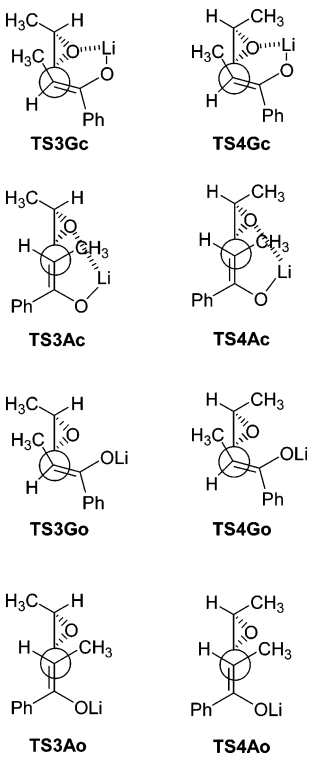

leading to γ-HK **3** (**TS3Gc**, **TS3Ac**, **TS3Go**, and **TS3Ao**) and the others leading to γ-HK **4** (**TS4Gc**, **TS4Ac**, **TS4Go**, and **TS4Ao**), with the appropriate corresponding nomenclature, are shown in Scheme 2. A systematic calculation was made of the electronic (solvent and vacuum) and free energy (vacuum) of all eight transition states, using the B3LYP/6-31+G(d)//B3LYP/6-31+G(d) theory level. The results obtained in vacuo are summarized in Table 2 and depicted in Scheme 3, where corrected free energies are used and **7a** and **7b** are the minima structures related to each TS examined (see below Figures 2 and 3 and corresponding text). An examination of the corrected free energy content differences ($\Delta G^{\#}_{rel}$), that is the difference between the corrected free energy of the TS of entry 1, Table 2 (**TS3Gc**) and the corresponding corrected free energy of the TS under examination, indicates that the chelated structure **TS3Gc** is the most favored one (see $\Delta G^{\#}_{rel}$ Table 2). The lower free energy of the chelated structures **TS3Gc**, **TS3Ac**, **TS4Gc**, and **TS4Ac** with respect to the open structures **TS3Ao** and **TS4Ao**, is reasonably due to the stabilizing effect of the coordination between the enolate and oxirane oxygens through the Li^+ (Scheme 2 and Figure 1), which is absent in **TS3Ao** and **TS4Ao**. The gauche **TS3Go** and **TS4Go** turned out to be less energetic than the corresponding anti **TS3Ao** and **TS4Ao** by 4.64 and 6.24 kcal mol^{-1}, respectively (entries 3−4 and 7−8, Table 2). This is probably due to Li^+ which, in **TS3Go** and **TS4Go**, is favorably shielded by the lone pairs of the enolate oxygen and to a certain extent by some C−C and C−H σ bonds[12] of the epoxide unit. On the contrary, in the case of **TS3Ao** and **TS4Ao**, the lithium cation is shielded practically only by the lone pairs of the enolate oxygen. Evidence of the above-mentioned interactions involving Li^+ can be obtained from the second-order perturbation theory analysis of the Fock matrix in NBO (Natural Bond Orbitals) reported in Table 3 (Supporting Information).[13]

Interestingly, **TS3Go** and **TS4Go**, where only weak Li^+-mediated interactions between enolate **1** and epoxide **2** are present (see above), have a free energy close to those

(12) The interaction between a transition metal center and a C−H bond is commonly referred to as "agostic interaction": (a) Brookhart, M.; Green, M. L. *J. Organomet. Chem.* **1983**, *250*, 395. (b) Schneider J. J. *Angew. Chem., Int. Ed. Engl.* **1996**, *35*, 1068. The "agostic interaction" was observed with lithium cation, as well: (c) Uhl, W.; Laya, M.; Massa, W. *Chem. Ber.* **1991**, *124*, 1511. (d) Hiller, W.; Laya, M.; Uhl, W. *Angew. Chem., Int. Ed. Engl.* **1991**, *30*, 324. The interaction between a transition metal and the C−C bond of cyclopropane has previously been observed: Hinrichs, R. Z.; Schroden, J. J.; Floyd Davis, H. *J. Am. Chem. Soc.* **2003**, *125*, 860.

(13) The second-order perturbation theory analysis of the Fock matrix in NBO basis for **TS4Ao** revealed three main interactions between orbitals (see Table 3, Supporting Information): two interactions due to LP*Li with two lone pairs of the enolate oxygen (the corresponding delocalization energy $E2$ is 6.79 and 2.75 kcal mol^{-1}, respectively, entries 10 and 11, Table 3, Supporting Information) and one between the RY*(2)Li with the remaining lone pair of the enolate oxygen (the corresponding $E2$ is 2.06 kcal mol^{-1}, entry 12, Table 3, Supporting Information). The same analysis repeated on **TS4Go** showed, in addition to the interactions with the lone pairs of the enolate oxygen ($E2$ of the most important is 11.26 and 4.86 kcal mol^{-1}, respectively, entries 1 and 4 Table 3, Supporting Information), three other stabilizing LP*Li interactions with C(12)−H(27), C(15)−H(30), and C(12)−C(14) σ bonds with a delocalization energy of 5.38, 2.72, and 2.20 kcal mol^{-1} respectively (entries 8, 9, and 7, Table 3, Supporting Information). A similar consideration can be made for the transition states **TS3Go** and **TS3Ao** (entries 13−24, Table 3, Supporting Information).

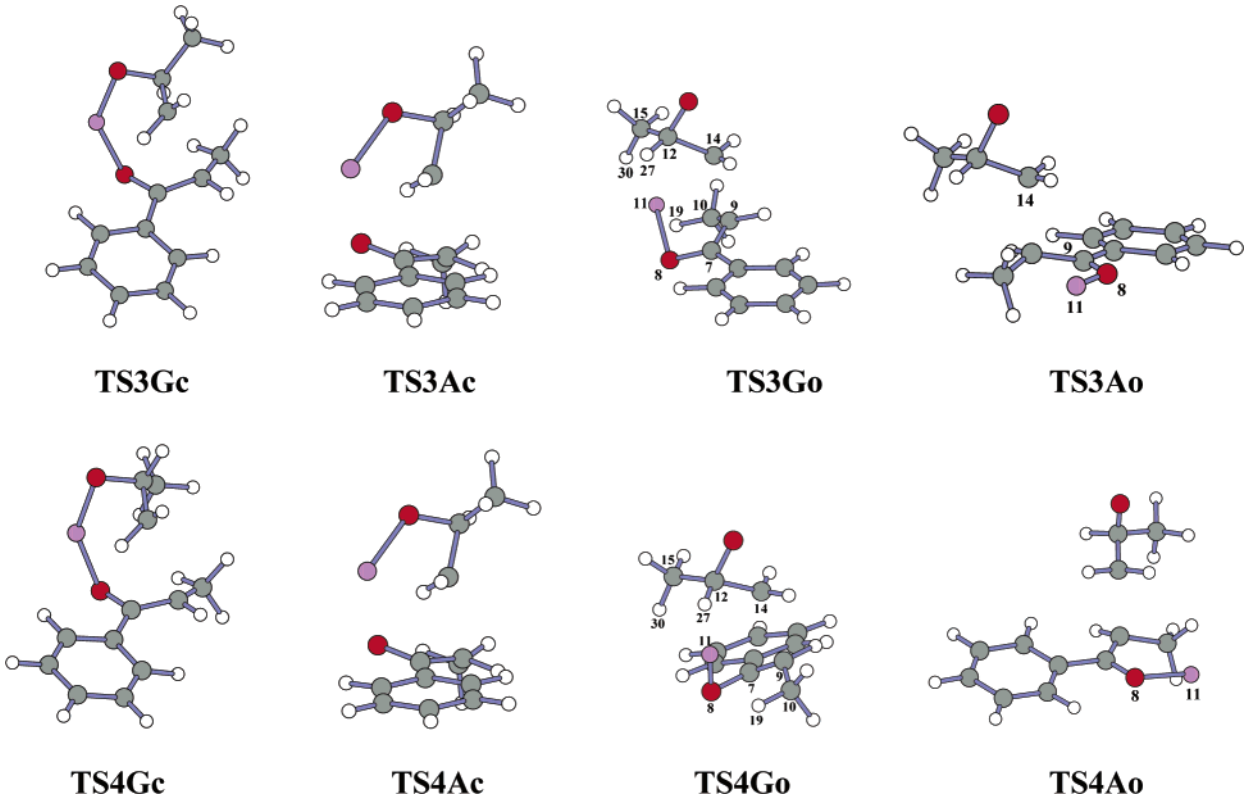

FIGURE 1. Transition states related to the addition reaction of enolate **1** to epoxide **2**.

SCHEME 3

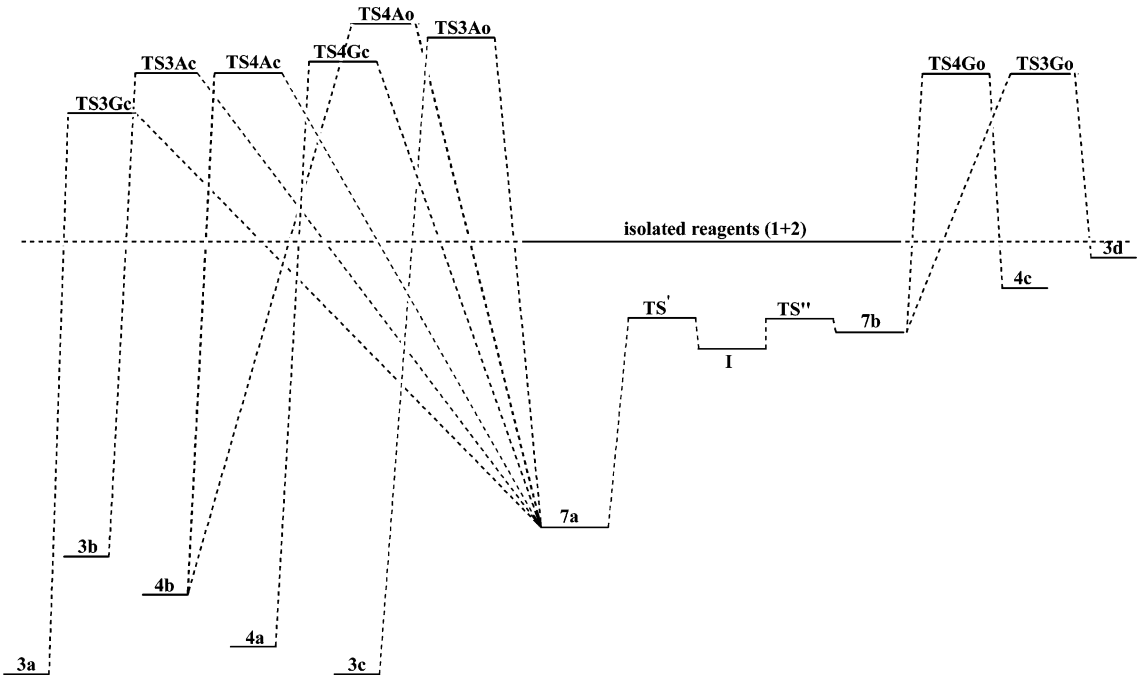

of the chelated structures **TS3Ac** and **TS4Ac**, where more stabilizing coordination bonds between Li^+ and the oxygens are present.

It was necessary at this point to calculate the corresponding minima related to all the transition structures considered, **TS3Gc**, **-Ac**, **-Go**, **-Ao** and **TS4Gc**, **-Ac**, **-Go**, **-Ao** (Scheme 3). The reagents' corresponding minimum related to all the chelated transition structures **TS3Gc**, **TS3Ac**, **TS4Gc**, and **TS4Ac**, turned out to be the complex **7a** (Figure 2), where a chelation between enolate **1** and epoxide **2** through Li^+ is present, as well. The free energy difference between **7a** and the calculated level, taken as a reference point, relative to the isolated noninteracting reagents (epoxide **2** and enolate **1**, dotted line, Scheme 3), is -26.93 kcal mol^{-1} ($K_{inst} = 1.803 \times 10^{-20}$), which is a measure of the free energy gain due to

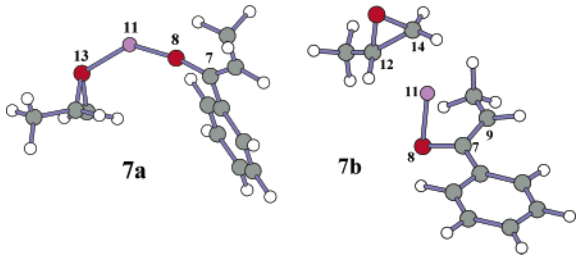

FIGURE 2. Complexes **7a** and **7b**, as minima corresponding to the reagents.

the coordination of the metal with both the oxygens of the enolate and oxirane ring (entry 11, Table 2). The situation in the open structures **TS3Ao** and **TS4Ao** is more complicated. We tried to perform a scan on the PES related to **TS3Ao** at the B3LYP/6-31+G(d) level**.** However, it was not possible to reach a stable minimum where both enolate **1** and epoxide **2** were isolated, not interacting reagents.[14] As a consequence, also **TS3Ao** and **TS4Ao**, in which there is no interaction between the enolate and epoxide through the Li^+, relax to complex **7a**. The lack of a stable minimum, where epoxide **2** and enolate **1** are isolated, not interacting species, increases, with respect to an hypothetical direct pathway, the free activation energy of the addition pathway of enolate **1** to epoxide **2** through the open TSs **TS3Ao** and **TS4Ao** by +26.93 kcal mol^{-1}. This value corresponds to the free energy difference between the energy level of complex **7a** and the corresponding one of the isolated reagents (entry 11, Table 2, and Scheme 3).[15]

The minimum corresponding to reagents, related to **TS3Go** and **TS4Go**, is complex **7b** (Figure 2 and Scheme 3). The free energy gain of complex **7b** with respect to the level corresponding to the isolated reagent is only −9.67 kcal mol^{-1} ($K_{inst} = 8.16 \times 10^{-8}$) (entry 12, Table 2). As a consequence, the corresponding activation free energy is only +27.79 and +27.66 kcal mol^{-1} for **TS3Go** and **TS4Go**, respectively (entries 3 and 7, Table 2). The higher free energy of complex **7b** (Figure 3) with respect to complex **7a** ($\Delta G_{\mathbf{7b-7a}} = +17.26$ kcal mol^{-1}) could be explained by the presence in **7a** of a Li^+-mediated coordination with both the enolate and the oxirane oxygen, which is absent in **7b**, where only weak interactions between Li^+ and some σ bonds of epoxide **2** are present, as discussed above in the case of **TS4Go** and **TS3Go** (Figures 2).[12] The results of second-order perturbation theory analysis of the Fock matrix in the NBO basis of complexes **7a** and **7b** are reported in Table 3.[16] The interconversion of complex **7a** to **7b** takes place through an intermediate **I** (entries 9 and 10, Table 2, and Scheme 3) and not through the isolated reagents. The activation free energy of the rate-limiting step of the transformation of complex **7a** into complex **7b** is the formation of intermediate **I** (+18.38 kcal mol^{-1}) (entry 9, Table 3). In Scheme 3 and in Figure 3, the minima corresponding to products are reported. The free energy of these minima is related to the Li^+ position with respect to the carbonyl and alcoholate functionalities. The conformers **3a**, **3c**, and **4a**, related to **TS3Gc**, **TS3Ao**, and **TS4Gc**, respectively, in which the Li^+ is engaged in coordination bonds with the oxygens of the carbonyl and the alcoholate groups, show the lowest free energy, confirming the stabilizing effect of chelation. An intermediate situation corresponds to the structures **3b** and **4b**, related to **TS3Ac** and **TS4Ac**, respectively, where the Li^+ is close to the alcoholate and so far from the carbonyl group that no chelation between the two oxygens through Li^+ is possible. The higher free energies correspond to structures **3d** and **4c**, related to the gauche **TS3Go** and **TS4Go**, respectively. In this case the Li^+ is far from the alcoholate moiety and close to the carbonyl group. This unfavorable situation involves an endothermic step for the formation of the new C−C bond between enolate **1** and epoxide **2** (entries 3 and 7, Table 2). However, in the reaction medium, this cation can easily be shifted near the alcoholate and, consequently, structures **3d** and **4c** can be converted to more stable conformers. To quantify the effect of chelation on the activation free energy content, the geometry of all the above-discussed TSs (**TS3Gc**, **-Ac**, **-Go**, **-Ao** and **TS4Gc**, **-Ac**, **-Go**, **-Ao**) was analyzed on the basis of two factors that may reasonably be supposed to be important in determining the activation free energy for the reaction of enolate **1** to epoxide **2**: (i) an appropriate alignment of all the forming and breaking bonds during the reaction pathway from reagents to products (stereoelectronic factors) and (ii) the steric interactions between the methyl groups of the interacting epoxide and enolate (steric factors). In the starting epoxide **2** and enolate **1**, the hybrid orbitals that are involved in the TS are considered (Figure 4).

The reasonably ideal situation is reached when the hybrid orbital of C(4) involved in the σ^* C(4)−O(6) lies in the same direction as the *p* orbital of C(3) involved in the π bond of the enolate. Four geometrical parameters, related to the stereochemical factors, can be identified, to have a simple measure of how far each structure is from the ideal situation described above: angle α [C(5)−

(14) The electronic energy profile of the **TS3Ao** PES presents a sharp decrease in the gradient in the proximity of the −624.294879 au value in vacuo, corresponding to a distance of 3.74 Å between the oxirane carbon C(14) and the enolate carbon C(9) involved in the bond formation, and −624.310943 au in the presence of the solvent (toluene/hexane, $\epsilon = 2.104$), corresponding to a 4.01 Å distance between the same carbons (see Figure 1). Whereas the electronic energy value in vacuo is lower than the corresponding value calculated for the isolated reagents by 2.39 kcal mol^{-1}, in the presence of the solvent (toluene/hexane), because of the better stabilization of the isolated reagents, this value rises by +7.74 kcal mol^{-1}. A frequency calculation of this point, in vacuo and in the presence of the solvent, showed an imaginary frequency and therefore its nature of "false minimum". After this value, the gradient rapidly increases and the structure collapses to the **7a** complex.

(15) If this minimum existed, it would mean that we are in the presence of a reaction pathway where the formation of the new C−C bond is characterized by a free activation energy of only +22.77 kcal mol^{-1}, which is the difference between the real $\Delta G^{\#}$ (+49.70 kcal mol^{-1}) and the ΔG of complex **7a** with respect to the isolated reagents (+26.93 kcal mol^{-1}), with the result that the rate-limiting step of the addition reaction would be the breaking of the **7a** complex.

(16) The second-order perturbation theory analysis of the Fock matrix in the NBO basis of complex **7a** revealed three principal interactions, one between LP*(1)Li and the LP(1) of the enolate oxygen (the delocalization energy *E*2 is 12.29 kcal mol^{-1}), and the others between the LP*Li and the two LPs of the epoxide oxygen (*E*2 is 5.90 and 6.03 kcal mol^{-1}) (entries 32, 34, and 35, Table 3, Supporting Information). The same analysis repeated on complex **7b** shows the interactions of LP*(1)Li with the lone pairs of the enolate oxygen, the most important with LP(1) (*E*2 is 10.10 kcal mol^{-1}, entry 28, Table 3), and some interactions between LP*Li and σ bonds, the largest ones with C(7)−C(8), C(7)−C(9), C(12)−C(14), and an interaction between LP*Li and the π-bond C(7)−C(9) (the delocalization energies are 3.73, 3.99, 3.24, and 2.65 kcal mol^{-1}, respectively (entries 25−27 and 29, Table 3, Supporting Information).

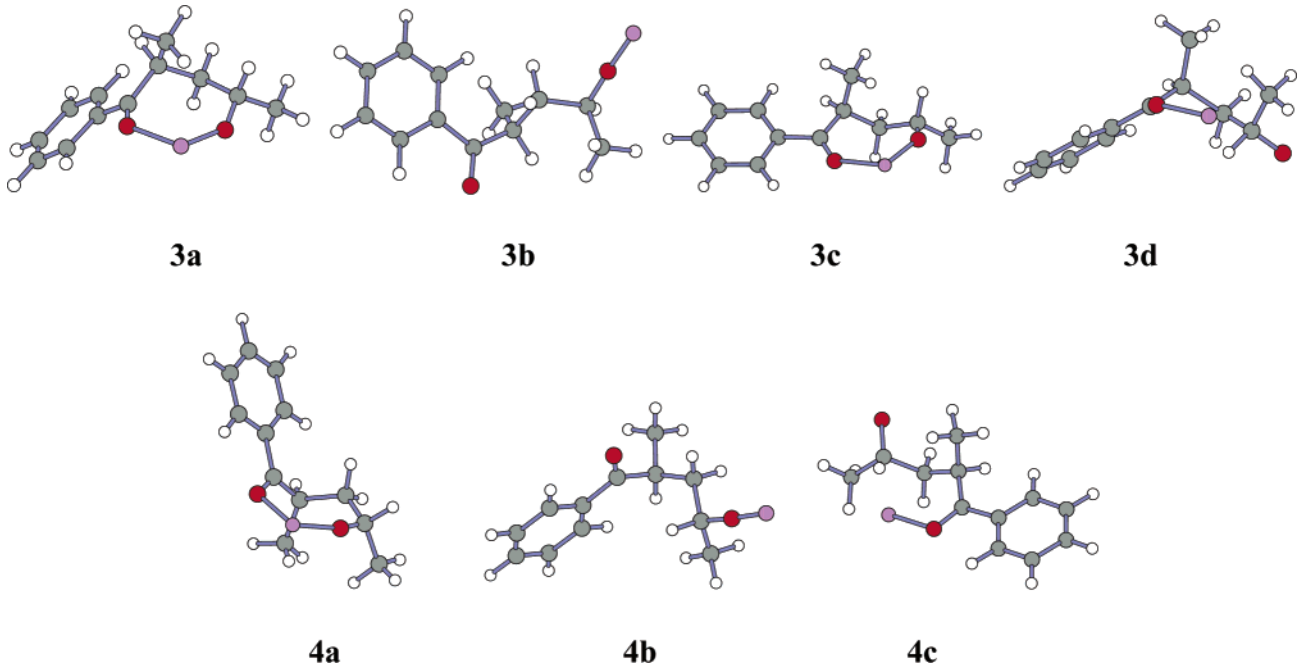

FIGURE 3. Minima corresponding to products related to the transition structures examined.

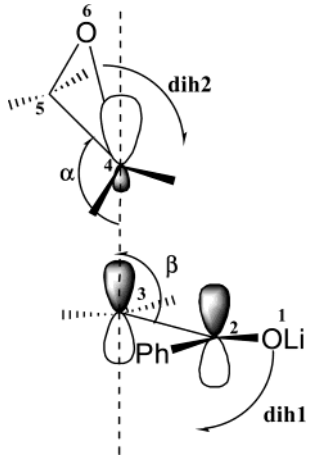

FIGURE 4. Representation of angles **α** and ***β*** and dihedral angles **dih1** and **dih2**: **α** = C(3)−C(4)−C(5) (range 100−190°), ***β*** = C(2)−C(3)−C(4) (range 0−180°); **dih1** = C(1)−C(2)−C(3)−C(4) (range 0−180°), **dih2** = C(3)−C(4)−C(5)−O(6) (range ±90−180°).

C(4)−C(3)], angle ***β*** [C(2)−C(3)−C(4)], dihedral angle **dih1** [C(1)−C(2)−C(3)−C(4)] and dihedral angle **dih2** [C(3)−C(4)−C(5)−C(6)]. Angle **α** is the angle between the oxirane C(4)−C(5) bond and the forming C(3)−C(4) bond: its ideal value is about 100° (calculated by NBO analysis of propene oxide on optimized B3LYP/6-31+G(d) geometry). Angle ***β*** indicates the bending of the C(3) *p* orbital: its ideal value is 90°. Dihedral angle **dih1** indicates the deviation of the enolate π bond with respect to the line connecting the C(2)−C(3) centers, whereas **dih2** indicates the rotation of the oxirane plane with respect to the enolate π bond plane; their ideal values are 90° and 180°, respectively. All these factors can be linearly combined into a coefficient *W*, which allows an easier comparison of the resultant of these stereoelectronic effects among the TS structures examined. The value $W = 0$ corresponds to quite a low activation free energy, which we consider close to zero as a first approximation, that is, to a situation in which the TS and the reagents, arranged with an appropriate orbital orientation, have the same geometrical parameters. The more the geometry differs from the ideal orientation of the reagents, the higher the *W* coefficient value is (Table 4, Supporting Information).

$$W = \frac{|\alpha - 100| + |\beta - 90| + (|\mathbf{dih1}| - 90) + |(|\mathbf{dih2}| - 180)|}{90}$$

As regards the steric factors, the value of the distance ***d*** (Å) between the carbons of the methyl group of enolate **1** and epoxide **2** constitutes a reasonable corresponding measure (Table 4, Supporting Information). An examination of Table 4 (Supporting Information) shows that an increase in the *W* coefficient value determines a corresponding increase in the activation free energy $\Delta G^{\#}$ for the reaction,[17] and that higher values of the *W* coefficient correspond to the chelated structures (Table 4, Supporting Information). In **TS3Ac**, **TS4Gc**, and **TS4Ac** (entries 2−4, Table 4, Supporting Information), for which the *W* value is >1, the corresponding $\Delta G^{\#}$ values are +44.98, +46.47, and +45.26 kcal mol^{-1}, respectively. The small differences between these $\Delta G^{\#}$ values could be due to steric interactions between the methyl groups. The highest activation free energy (+46.47 kcal mol^{-1}) is found in **TS4Gc**, where the distance between the methyls is the smallest (***d*** = 3.28 Å, entry 3, Table 4, Supporting Information). **TS3Gc**, for which the *W* coefficient is 0.862,

(17) For a better comprehension of the coordination effect of Li^+ on the activation free energy (vacuum) and activation electron energy (solvent), in the case of the nonchelated transition states **TS3Ao** and **TS4Ao** (entries 6 and 8, Table 4, Supporting Information), the isolated reagents, instead of complex **7a**, was considered the minimum. The corresponding extrapolated $\Delta G^{\#}$ (vacuum) and $\Delta Ee^{\#}$ (solvent) are reported in italics and the real value in brackets.

SCHEME 4

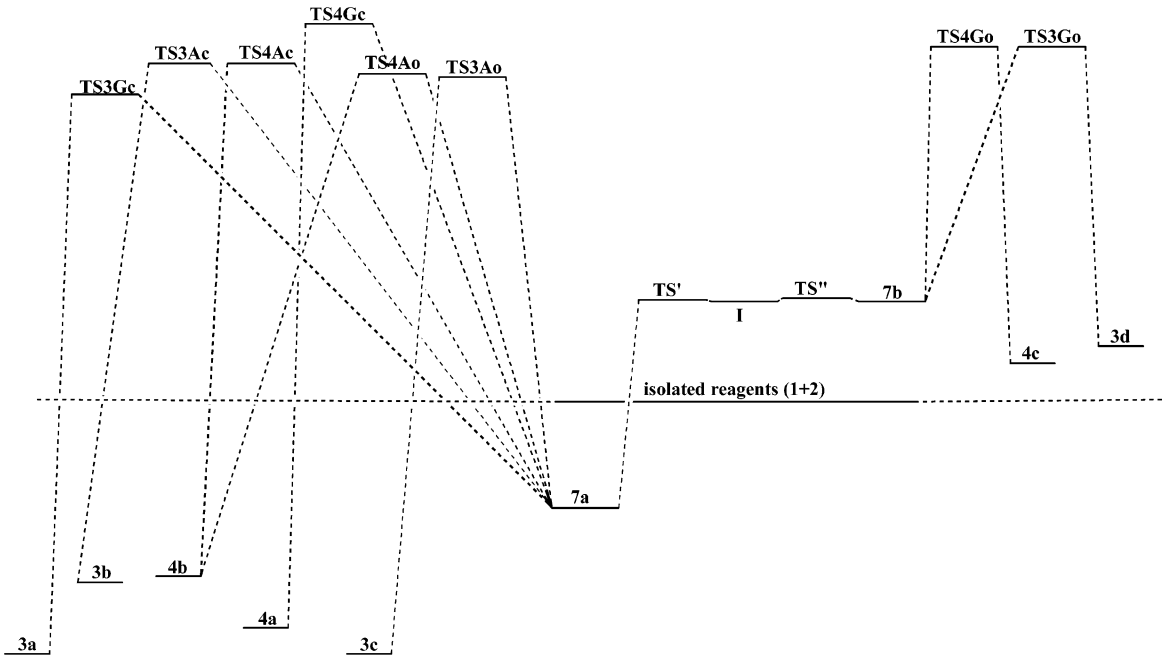

is the favored chelated transition structure (entry 1, Table 4, Supporting Information). In this case the angle **α** is close to the ideal value, to the point that the negative contribution to the *W* coefficient is principally due to the dihedrals **dih1** and **dih2**. As for the open structures **TS3Ao** and **TS4Ao** (entries 6 and 8, Table 4, Supporting Information), the *W* coefficient values are the lowest (0.327 and 0.390, respectively) and are almost close to the ideal behavior ($W = 0$), with the corresponding extrapolated $\Delta G^{\#}$ values +22.77 and +24.23 kcal mol^{-1}.[17] In the case of **TS3Go** and **Ts4Go**, the weak Li^+-mediated interactions between enolate **1** and epoxide **2** (entries 5 and 7, Table 4, Supporting Information) determine only a modest increase in the *W* coefficient (0.536 and 0.627, respectively), compared with **TS3Ao** and **TS4Ao**, due principally to a modest variation of **α** and **dih1** values, which is reflected in an increase of $\Delta G^{\#}$, +27.79 and +27.66 kcal mol^{-1}, respectively (entries 5 and 7, Table 4, Supporting Information). **TS4Go** is somewhat less energetic than **TS3Go** despite its greater *W* value, probably because of a reduced steric interaction between the two methyl groups (see ***d*** values, 4.81 and 3.70 Å, respectively, entries 5 and 7, Table 4, Supporting Information).

The results obtained (Table 4, Supporting Information) indicate that a higher activation free energy corresponds to a stronger interaction between enolate **1** and epoxide **2** (chelated structures). Any interaction stabilizes the minima more than the transition structures, because it determines some distortion in the TS from the ideal alignment of the orbitals, as discussed above, with a corresponding increase in the $\Delta G^{\#}$. As a consequence, the reaction pathways through the completely open structures **TS3Ao** and **TS4Ao**, which have the lowest *W* coefficient values and show no interaction between lithium enolate and epoxide, would be favored (Scheme 3). However, no corresponding minimum was found for these structures, where Li^+-mediated interactions between enolate and epoxide are not present (as in the isolated reagents). All this makes the pathways through **TS3Go** and **TS4Go** giving γ-HK **3** and **4** the most favored, on the basis of our results. Evidently the weak stabilization of Li^+ by the σ bonds, found in **TS3Go** and **TS4Go**, stabilizes the reagents in the form of complex **7b**, which is a real minimum and, at the same time, determines only a weak influence on the stereoelectronic factors, compared with all the chelated TS structures. This is particularly evident from a comparison of the free energies of the open structures **TS3Go** and **TS4Go** with those of the chelated structures **TS3Ac** and **TS4Ac** (entries 2, 3, 6, and 7, Table 2). The energy gain, due to the chelation, present in **TS3Ac** and **TS4Ac**, which is greater than that one due to the weak Li^+-mediated interactions, present in **TS3Go** and **TS4Go**, is balanced by the more unfavorable stereoelectronic factors. As a consequence, **TS3Go**, **TS4Go**, **TS3Ac**, and **TS4Ac** have similar energy values.

To investigate whether the solvent had any significant effect on the above conclusions based on the studies conducted in vacuo, we performed an SP of all the in vacuum optimized structures in the presence of the solvent (hexane/toluene). The results obtained are reported in Table 2 and illustrated in Scheme 4, where the electronic energies are used. Furthermore, the absolute electronic energies in vacuo (Ee_{vac}) and in the presence of the solvent (Ee_{solv}) and the corresponding differences ($Ee_{solv} - Ee_{vac}$) are reported in Table 5 (Supporting Information). The $\Delta Ee^{\#}_{rel}$ does not show significant differences (<1 kcal mol^{-1}) with respect to the results obtained in vacuo except for **TS3Ao** and **TS4Ao**, where this value decreases from +11.23 to +2.03 kcal mol^{-1} and from +12.47 to +3.12 kcal mol^{-1}, respectively (entries 4 and 8, Table 2). The solvent stabilizes **TS3Ao** and **TS4Ao** more than the other structures (see $Ee_{solv} - Ee_{vac}$, entries 1−8, Table 5, Supporting Information). In these structures, Li^+ is not involved either in the chelation or in agostic interactions, with the result that it is more available for dipole−dipole interactions with the solvent.

As a consequence, the $\Delta Ee^{\#}$ for the pathways which involve **TS3Ao** and **TS4Ao** decreases by about 8.5 kcal mol^{-1} (entries 4 and 8, Table 2), but this value is not sufficient to make these pathways the preferred ones. In fact, also in the presence of the solvent, the minimum corresponding to **TS3Ao** and **TS4Ao** is complex **7a**. The scan on the PES related to **TS3Ao** shows a behavior similar to that found in vacuo.[14] In this framework, an examination of Table 2 indicates that also in the presence of the solvent, the pathways involving **TS3Go** and **TS4Go** are the most favored ones (entries 3 and 7).

The reference point corresponding to the isolated reagents is so stabilized by the solvent that the ΔEe for the formation of complexes **7a** and **7b** increases from −21.85 (vacuum) to −9.71 kcal mol^{-1} (solvent) and from −5.41 (vacuum) to +9.04 kcal mol^{-1} (solvent), respectively (see entries 9 and 10, Table 2 and Scheme 4). As a consequence, the interconversion of complex **7a** into complex **7b** probably takes place through the isolated reagents and not through the intermediate **I**. The larger contribution to the stabilization of the isolated reagents is due to the solvation of enolate **1** (see entries 11 and 12, Table 5, Supporting Information).

The stabilization due to the solvation of Li^+, in the absence of chelation or other stabilizing effects, for example, agostic interactions, is also evident in the minima corresponding to products **3b** and **4b**: the better solvation of **3b** and **4b** (see Figure 3), with respect to **3a**, **3c**, and **4a** (entries 13−15 and 17−18, Table 5, Supporting Information) decreases the ΔEe of the reaction by about 5 kcal mol^{-1} (entries 2, 6, and 8, Table 2). A similar situation is found for products **3d** and **4c**, where the lithium is close to the carbonyl group and far from the alcoholate moiety (see Figure 3). In this case, the charge separation present in **3d** and **4c** benefits from the presence of the solvent (entries 16 and 19, Table 5, Supporting Information). As a consequence, the ΔEe for the pathways which involve **TS3Go** and **TS4Go** decreases from +5.25 to −2.67 kcal mol^{-1} and from +0.57 to −5.14 kcal mol^{-1}, respectively.

As for the relationship between the *W* coefficient and the activation energy (in the case of the solvent the electron activation energy was considered), another parameter was added to the stereoelectronic and steric factors. When the solvent stabilization is about the same for both reagents and corresponding TSs (this is the case of the pathways involving **TS3Gc**, **-Ac**, **-Go** and **TS4Gc**, **-Ac**, **-Go**), the relationship between the *W* coefficient and the activation electronic energy is maintained (entries 1−5 and 7, Table 4, Supporting Information). On the other hand, the extrapolated electronic activation energies[17] for pathways involving **TS3Ao** and **TS4Ao** are higher than those corresponding to the pathways involving **TS3Go** and **TS4Go**, despite the lower *W* coefficient. The reason is the better stabilization by the solvent of the isolated reagents, taken as a reference point, with respect to **TS3Ao** and **TS4Ao**.

Conclusions

In this paper, the different possible reaction pathways involving TSs for the addition reaction of monomeric lithium enolate derived from propiophenone (**1**) to propene oxide (**2**) are examined in vacuo and in the presence of the solvent (toluene/hexane). The anti nonchelated TS, previously hypothesized for this reaction, does not seem to be so probable. The lack of a minimum with an energy higher than the one corresponding to complex **7a** makes **TS3Ao** and **TS4Ao** the more disfavored (vacuum) and simply not favored (solvent) transition structures. On the other hand, the chelation process between the oxygens of the enolate and the epoxide through Li^+ stabilizes the reagents more than the TS structures, because it strongly affects the geometry of the transition state, thus increasing the corresponding $\Delta Ee^{\#}$ and $\Delta G^{\#}$ values. Also when the reaction solvent was considered, the situation did not change. The most probable pathway of the reaction involves a TS where the enolate **1** C=C and the epoxide **2** C−C bonds are in a gauche relationship and where Li^+ is stabilized by some C−C and C−H σ bonds of epoxide **2**. These interactions are sufficient to stabilize enolate **1** and epoxide **2** in a minimum (**7b**), in which there is no coordination between the two oxygens through Li^+, and, at the same time, they have a limited effect on the geometry of the corresponding transition states **TS3Go** and **TS4Go**, compared with the ideal behavior. Further studies on this reaction are in progress, with the aim of examining the possible incursion of dimers of enolate **1**.

Acknowledgment. This work was supported by the Università di Pisa, the Ministero dell'Università e della Ricerca Scientifica e Tecnologica (MURST), and Gaussian Inc. P.C. gratefully acknowledges Merck Research Laboratories for generous financial support deriving from the 2002 ADP Chemistry Award.

Supporting Information Available: Experimental details of the reaction of enolate **1** with epoxide **2**; *Z*-matrices, absolute energies, and other thermochemical data for all optimized structures: **TS3Gc**, **-Ac**, **-Go**, **-Ao**, **TS4Gc**, **-Ac**, **-Go**, **-Ao**, complexes **7a** and **7b**, enolate **1**, epoxide **2**, **TS′**, **TS″** and corresponding intermediate **I**, and reaction products **3a**−**d** and **4a**−**c** (Tables 2−5). This material is available free of charge via the Internet at http://pubs.acs.org.

JO034587M